

# VISCOUS AND WAVE DRAG OPTIMIZATION FOR A TRANSPORT AIRCRAFT MISSION ADAPTIVE WING

F.M. Catalano, P.C. Greco Jr - Aircraft Laboratory – University of São Paulo-Brazil  
A.L. Martins - EMBRAER, Brazil

**Keywords:** *Variable camber wing, drag reduction, optimization*

## Abstract

*A direct optimization study has been performed to produce a preliminary evaluation of the potential benefits of a mission adaptive wing employing variable camber technology in typical jet transport aircraft missions, in terms of fuel efficiency increase directly obtainable from airfoil viscous (pressure + friction) drag as well as wave drag reduction. The present work has been proposed as an extension of previous research [4-5]. Its main objective is a preliminary evaluation of the potential benefits of VCW technology to enhance the fuel efficiency of jet transport aircraft by wing airfoil viscous (pressure and friction) and wave drag reduction, at high speed, subsonic and transonic cruise flight conditions. The optimization objective function is set to maximize an integrated airfoil range parameter, considered to be representative of the maximum possible variation of aircraft range due to viscous and wave drag reduction. A 2-D airfoil analysis approach has been adopted, associated with a proposed idealized variable camber mechanism based on elastic deformation and surface extension. Using a direct function optimization program coupled to a viscous-inviscid airfoil analysis routine and a finite difference method to solve the transonic small disturbance (TSD) equation, optimized variable camber configurations were obtained for several of the decreasing weight conditions a typical transport aircraft faces along a cruise mission leg, due to fuel consumption. Independent runs have been executed considering only trailing and both leading and trailing edge camber variation and, for each of*

*them, an integrated range parameter has been obtained, proportional to the maximum possible aircraft range.*

## 2 Analysis and Optimization Methods

For the 2-D analysis of the airfoil viscous drag, the method by Williams [9] was adopted. The method uses an integral boundary layer method, extended to also calculate separated flow by assuming a two-parameter description of the separated velocity profiles. The program is of the semi-inverse type, in which a direct inviscid calculation is coupled to an inverse calculation of the boundary layer. The outer inviscid flow is assumed to be both incompressible and irrotational, so that it can be described by the relevant solution of Laplace's equation, which is obtained by a surface singularity method. In the inner viscous flow, the laminar portion of the boundary layer is calculated by Thwaites' method and natural transition is predicted using Granville's correlation.

During transonic flight the airfoil shape may be optimized to minimize shock wave drag. It is well known that shock strength and position can be strongly affected by small changes in airfoil shape. The transonic small disturbance (TSD) equation, derived from the full potential equation, is solved using a finite difference method to obtain the shock wave drag. A computer code, developed at the University of Kansas under the supervision of Dr. C. Edward Lan, solves the TSD equation in the frequency domain rather than in the time domain [12, 13, 14]. To achieve this, the time-dependent TSD equation is first separated into the in-phase and

out-of-phase components through a nonlinear harmonic averaging method. The equations then become similar in form to steady aerodynamic equations thus simplifying the problem. Corrections for nonisentropic and rotational flow are used to improve calculations in the shock region.

To control the overall optimization procedure, the optimizer program CONMIN, by Vanderplaats [10], was adopted. The program is coupled to the airfoil analysis routine, running it as a multivariable function evaluator. A chosen objective aerodynamic characteristic  $F$  (for example,  $M L/D$ ) is declared dependent of a chosen set of decision variables  $\{X_i\}$  (for example, VCW defining parameters). Using an iterative gradient method, the optimizer is able to numerically search for the set of decision variables values  $\{X_i\}_{opt}$  which returns the minimum (or maximum) value of the objective aerodynamic characteristic chosen. The final set of decision variables must be constrained to a certain domain by inequality equations, to ensure that the final result is feasible for the conditions required.

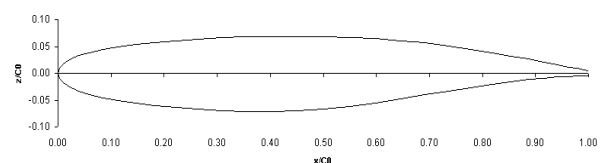
### 3 Variable camber wing representation model

An approach restricted to the two-dimensional airfoil domain has been chosen, representing a basic jet transport aircraft wing by a typical supercritical airfoil [6], displayed in Figure. 1

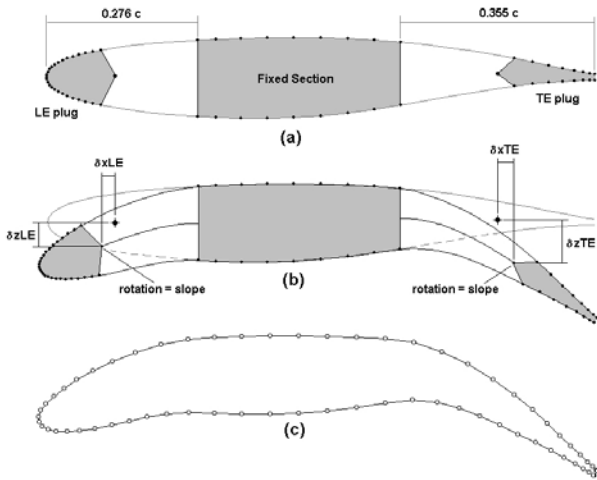
An *idealised* model for the camber variation mechanism was proposed due to the following factors: (a) the proposal of a really feasible VCW mechanism is considered far beyond the scope of this work, and also unnecessary for a preliminary evaluation; (b) A highly idealised mechanism would represent the outer envelope of possible solutions, that is, many possible “real world” VCW devices could be seen as some particular case, covered by the idealised model; (c) inexpressive benefits obtained with an idealised model would be a strong indication that a real mechanism would be even less effective, and possibly of no interest. Based on that, the idealised variable camber mechanism proposed is presented in

Fig. 2. As in previous VCW proposals [1-4], the mechanism assumes a central load carrying fixed section of the wing and two geometrically variable sections attached to it. Here the variable sections extend from the LE to 27.6% of the chord and from 64.5% of the chord to the TE (Figure 2a). The main idealisation assumption for the mechanism is that shape variation could be entirely achieved by elastic deformation and length extension of the upper and lower surfaces of the variable sections. For this, two regions on the variable sections are considered to be “plugs”, fixed in geometric shape to a certain extent of the chord from the LE and TE (Fig. 2a). Arbitrary shape variation is then obtained through the following procedure:

(a) Arbitrary displacement ( $\delta X$ ,  $\delta Z$ ) of LE and TE plugs, measured from an assumed reference point on each of them (“RP”, Fig.2b);  
 (b) Rotation of the plugs around the reference points. To keep minimum structural feasibility of the shape obtained, the rotation is assumed to be the slope of natural cubic spline curves, attached to the mean camber line of the central fixed section, and passing through each plug reference point (Fig. 2b); resampled airfoil representation by a single parametric cubic spline function, interpolating only the points on the LE and TE plugs and on the central fixed section. Fig. 2c shows an example resulting airfoil, discretized in 65 points and ready for aerodynamic analysis (Fig. 2c). The cubic spline representation is considered to closely reproduce the possible shape the flexible variable sections would assume, given a certain plug displacement and rotation configuration.



**Figure 1** Base Airfoil (Ref. 6)



**Figure 2** Idealized camber variation scheme:  
 (a) Undeformed base airfoil.  
 (b) Plug displacement and rotation.  
 (c) Airfoil shape resampling (65 points).

**4 The optimization problem**

Once a fixed geometry wing can be optimally designed for one set of weight and flight conditions only, transport aircraft usually cruise at off-design conditions. To evaluate the cruise weight variation effect on range, one must take the integral form of the range equation [7] for a jet aircraft, expressed by:

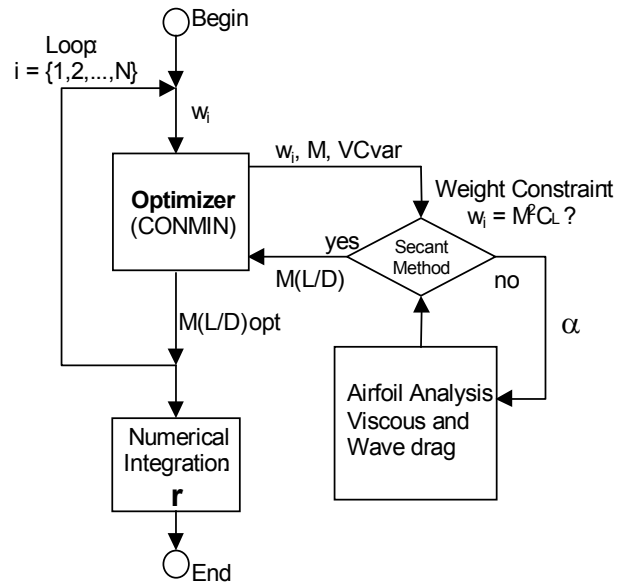
$$\frac{RC}{a} = r = \int_{W_N}^{W_1} M \frac{L}{D} \frac{dW}{W} \quad (1)$$

Where indexes 1 and N indicate conditions at the start and at the end of the cruise phase, respectively. It is evident that the maximization of the  $M(L/D)$  term at every point of the cruise leg maximizes the integrated range parameter  $r$  (**Figure 3**). Based on that, the optimization problem studied here can be stated with the following enunciate:

*Given a typical jet transport aircraft cruise mission, find the set of variable camber wing parameters that optimize (maximize) the  $M(L/D)$  term for every weight condition found within the  $W_1$  to  $W_N$  variation range, so maximizing the integrated range parameter  $r$ .*

(a) The present work considers the optimization of the wing alone, from the

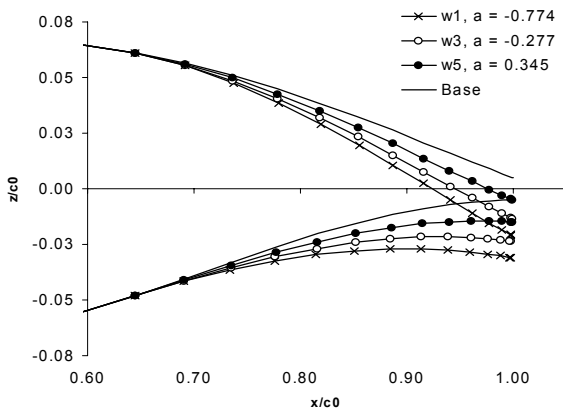
standpoint that such results would represent the maximum potential benefits the wing itself would be able to offer in terms of viscous and wave drag reduction, without considering eventual trade-offs with other sources of drag.



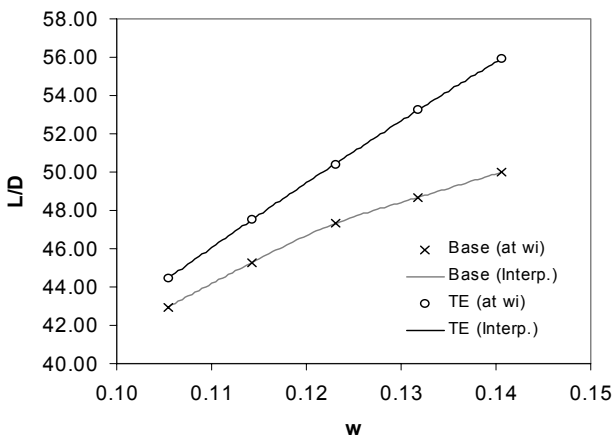
**Figure 3** Optimisation scheme

**5 Results and Discussion**

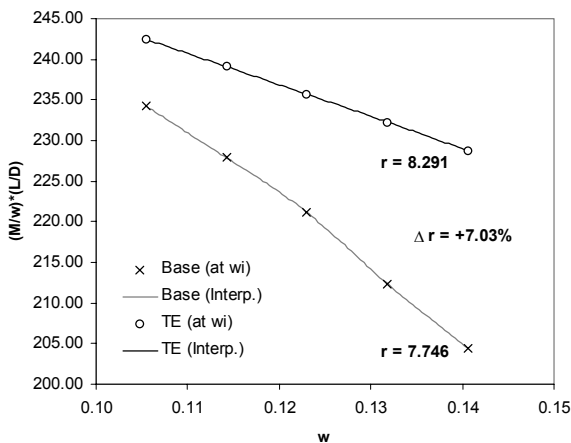
The resulting TE variable camber shapes obtained within the range defined is displayed in Figure 4. The gradual reduction of camber curvature from the highest weight  $w_1$  to the lowest  $w_5$  can be clearly observed, as well as the  $\alpha$  variation needed to cope with the weight constraint ( $w_i = M^2 C_L$ ). Figure 5 gives an indication of the  $L/D$  increase obtained with the geometry adaptation, in relation to the fixed airfoil. However, it is believed that the variation of the integrand term of the range equation  $M(L/D)/w$  (Equation. 1) in Figure 6 gives a clearer indication of what that efficiency increase means in terms of potential increase in integrated range parameter  $r$  (area below each curve). As indicated, an increase of  $\Delta r = +7.03\%$  is expectable.



**Figure 4** Optimized TE airfoil shapes and  $\alpha$  values, Case 1 (TE only).



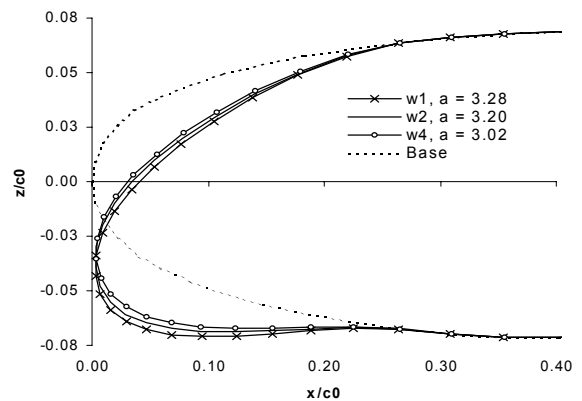
**Figure 5** L/D for base and Case 1 (TE only)



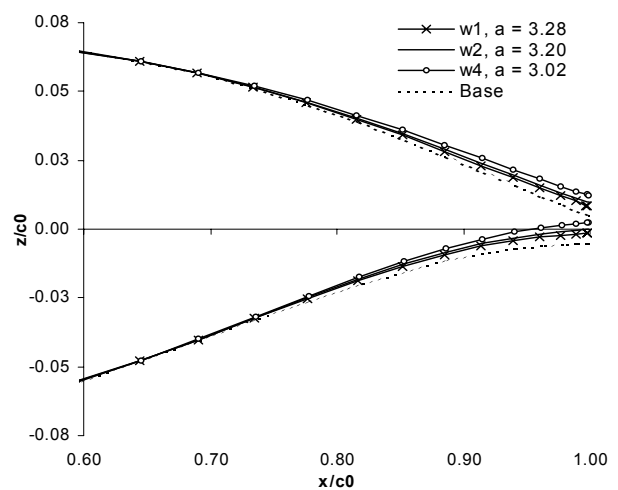
**Figure 6**  $M(L/D)/w$  for base Case 1 (TE only)

Fig. 7 and 8 present the resulting optimized geometries for the LE and TE simultaneously variable camber case, for three weight parameter values within the range

$[w_1, w_5]$ . The main feature evident in Figure 7 is the intense downward curvature at the leading edge, probably adapting the stagnation point around it to an ideal position. Also, a gradual reduction of LE curvature with reduction of weight is clearly seen. Less obvious is the upward curvature of the trailing edge, displayed in Figure 8, also gradually intensified by the increasing weight. Figure 9 presents the resulting L/D increase observed within  $[w_1, w_5]$ , clearly superior to both the base airfoil and the previous case. The correspondent curves of the  $M(L/D)/w$  range parameter integrand are displayed in Figure 10, indicating a variation  $\Delta r = 24.6\%$  over the base airfoil, adding a 16.4% increase over Case 1



**Figure 7** Optimised LE airfoil shapes and  $\alpha$  values, Case 2 (LE+TE).



**Figure 8** Optimized TE airfoil shapes and  $\alpha$  values, Case 2 (LE+TE).

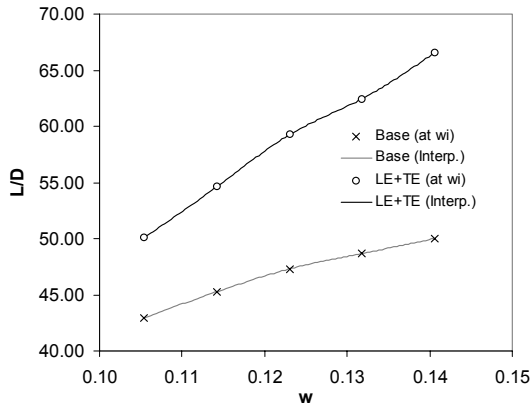


Figure 9 L/D for base and Case 2 (LE+TE)

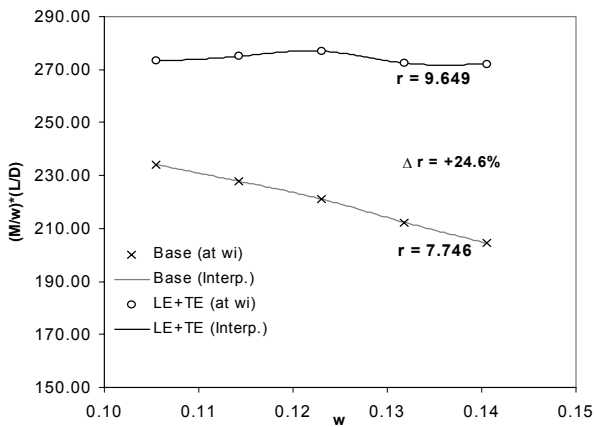


Figure 10  $M(L/D)/w$  for base and Case 2 (LE+TE)

Results in terms of pressure distributions are displayed in Figure 11, for the base airfoil and Case 1 and Case 2 optimized geometries, all for the highest loading condition. One first interesting feature observed is the shape of the pressure distribution for the Case 2 airfoil, where LE adaptation smoothes down the upper surface suction peak seen on the base airfoil, bringing it to a more downstream position along the chord, thus largely alleviating the  $C_p$  gradient after it. For the Case 1 airfoil, it is observed that a large suction peak reduction also occurs, although the unaltered LE curvature leaves it at roughly the same chordwise position. It can be seen that the Case 1 airfoil becomes “after-loaded”, with the expected pressure difference increase around the curved TE. Case 1 (TE only) tends to offer better transonic qualities than the base airfoil for the same condition. That is indicated in the flatter upper surface  $C_p$  distribution that is generated in Case 1, which lead to the formation of weaker

shocks (Figure 12). Comparing the base airfoil and the Case 1 optimized shape in Figure 11, it can be seen that the latter has the LE of the airfoil at a much favorable angle of attack, offering its upper surface less deviated from the freestream. In summary, the observations made indicate that, under real supercritical cruise constraints, LE variable camber deflections are expected to be much less intense than the ones observed for Case 2.

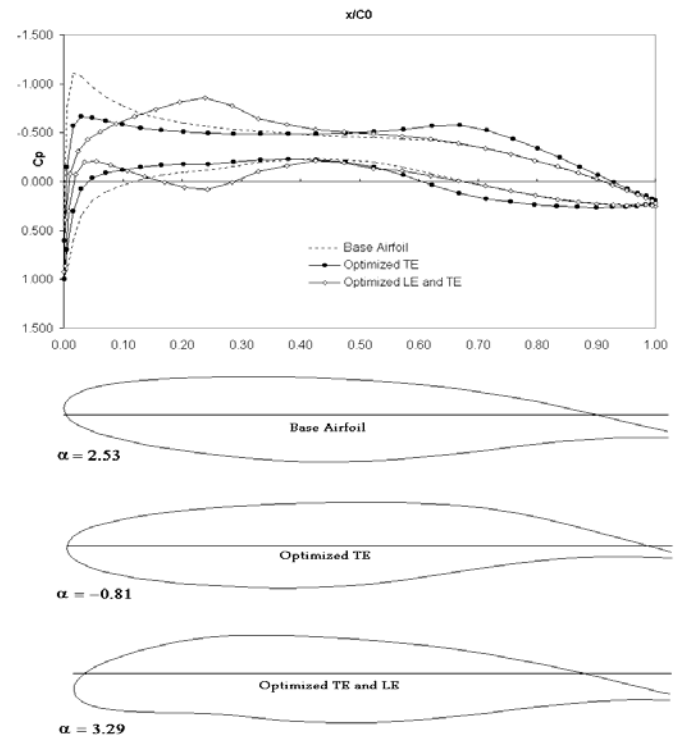


Figure 11  $C_p$  values and profiles for base and optimized airfoils (rotated by  $\alpha$ ).

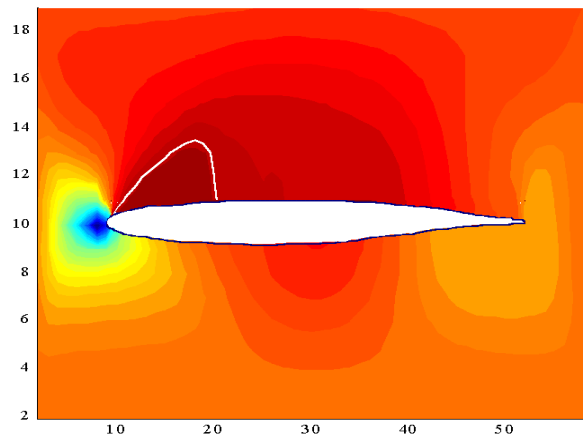


Figure 12 Mach contours for Case 1

## References:

- [1]. Powers, S.G.; Webb, L.D.: Flight Wing Surface Pressure Measurements and Boundary-Layer Data from the F-111 Smooth Variable-Camber Supercritical Mission Adaptive Wing. *NASA TM 4789*, 1997.
- [2]. Gilyard, G.; España, M.: On the Use of Controls for Subsonic Transport Performance Improvement: Overview and Future Directions. *NASA TM 4605*, 1994.
- [3]. Fielding, J. P.; Varziry-Zanjany, M.A.F.: Reliability, Maintainability and Development Cost Implications of Variable Camber Wings. *Aeronautical Journal*, May, 1996. p. 183-195
- [4]. Martins, A.L.; Catalano, F.M.: Aerodynamic Optimization Study of a Mission Adaptive Wing for Transport Aircraft. *20<sup>th</sup> ICAS*, Italy, 1996.
- [5]. Martins, A.L.; Catalano, F.M.: Viscous Drag Optimization For A Transport Aircraft Mission Adaptive Wing *21<sup>th</sup> ICAS 98*, Australia, 1998.
- [6]. McKinnon, A.V.: An Experimental Study of a Variable Camber Wing. *Ph.D. Thesis, Cranfield Institute of Technology*, UK, October, 1993.
- [7]. Raymer, D.P.: Aircraft Design: a Conceptual Approach. *AIAA Education Series*, 1989.
- [8]. Torenbeek, E.: Synthesis of Subsonic Airplane Design. *Delft University Press*, 1982.
- [9]. Williams, B.R.: The Prediction of Separated Flow Using a Viscous-Inviscid Iteration Method. *R.A.E. Tech. Memo. Aero 2010*, 1984.
- [10]. Vanderplaats, G. N.: CONMIN - A FORTRAN Program for Constrained Function Minimization. *NASA TM X-62282*, Ames Research Center, 1973.
- [11]. Goldberg, D. E.: Genetic Algorithms in Search, Optimization and Machine Learning. *Addison-Wesley*, 1989.
- [12]. Hwang, H., Computation of Unsteady Transonic Flow About Airfoils in Frequency Domain Using the Full-Potential Equation, *Ph.D. Dissertation, The University of Kansas*, 1988.
- [13]. Sun, T. H., Unsteady Transonic Aerodynamics in Frequency Domain for Flutter Analysis, *Ph.D. Dissertation, The University of Kansas*, 1991.
- [14]. Greco, P. C., Jr., Lan, C. E. and Lim, T. W., "Frequency Domain Unsteady Transonic Aerodynamics for Flutter and Limit Cycle Oscillation Prediction," *35<sup>th</sup> AIAA Aerospace Sciences Meeting and Exhibit, Paper No. 97-0835*, Reno, NV, January 1997.